Supporting Information

Simple analytical expression for the peak-frequency shifts of plasmonic resonances for sensing

Jianji Yang[1], Harald Giessen[2] and Philippe Lalanne*[1]

[1] Laboratoire Photonique Numérique et Nanosciences, Institut d'Optique d'Aquitaine, Univ. Bordeaux, CNRS, 33405 Talence, France.

[2] 4th Physics Institute and Research Center SCoPE, University of Stuttgart, Pfaffenwaldring 57, 70550 Stuttgart, Germany.

* E-mail: Philippe.lalanne@institutoptique.fr

Content of the document

(1) Comparison of the present master equation eq 1 in the main text with a quasi-static formula recently published [1]

(2) Analysis of the errors resulting from the approximations made to derive the master equation eq 1 (main text)

1. Comparison of the present Master Equation with the quasi-static Formula

A formula for predicting frequency shifts of resonances of plasmonic nanoresonators was recently reported in eq 11 in Ref [1]. With the same notation as in Ref [1], it reads as

$$\Delta\omega_m = -\alpha_{NP}\frac{\mathrm{d}\omega}{\mathrm{d}\varepsilon_{ca}}\frac{\left|\mathbf{E}_m(\mathbf{r}_{NP})\right|^2}{\iiint_{\text{cavity}}\left|\mathbf{E}_m(\mathbf{r})\right|^2\mathrm{d}^3\mathbf{r}}, \qquad \text{(S1)}$$

where α_{NP} and ε_{ca} denote the polarizability of the perturbation (assumed to be infinitely small and placed at $\mathbf{r}_{NP}$) and the permittivity of the metallic resonator respectively. The integral in the denominator runs over the metallic resonators. Referring to ref [1], the field $\mathbf{E}_m$ is defined as the field scattered by the metallic resonator under plane-wave illumination at the *real-valued* resonance frequency ω_m. Strictly speaking this field is not the same as the resonance mode (the quasi-normal mode) that is used in our work, which is defined with a complex frequency. Hereafter, following [1] we will use the scattered field $\mathbf{E}_m$ to evaluate eq (S1) and refer to eq (S1) as *quasi-static formula*, since it is derived using quasi-static approximation.

A weakness of the quasi-static theory is that it is valid only at deep sub–λ scales. In this Section, using fully-vectorial calculations, we compare the accuracy of our present master equation (eq 1 main text) and the quasi-static formula, for metallic resonators with progressively increasing sizes.

However, before starting any comparison, we first check that we are correctly implementing eq (S1) by reproducing some of the results in [1]. For that purpose, we consider three resonators, a silver ellipsoid (40-nm long axis, 14-nm short axes), a silver nanorod dimer (arm size 28 nm x 10 nm x 10nm, 10-nm gap), and a silver split-ring resonator (10 nm x 10 nm wire cross-section, 32 nm x 30 nm outer dimension of the ring, 10 nm gap). These geometries are the same as those used in Fig. 2 in [1]. For each geometry, we calculate the exact complex frequency shift $\Delta\tilde{\omega}_{\text{exact}}$ as the difference between the complex eigenfrequencies of the perturbed and the unperturbed one (see the main text) and define $\Delta\omega_{\text{exact}} = Re\left(\Delta\tilde{\omega}_{\text{exact}}\right)$. Following [1], we consider a tiny silicon nanosphere as the perturbation. We calculate the scattered field $\mathbf{E}_m$ is with COMSOL and denote the predicted shift by $\Delta\omega_{\text{predict}}$.

In Fig. S1, we plot $\Delta\omega_{\text{exact}}$ as a function of $\Delta\omega_{\text{predict}}$ for the three resonators and for different perturbation locations (see the caption). As in Ref [1], we plot the line $\Delta\omega_{\text{exact}} = 1.07\Delta\omega_{\text{predict}}$ (black line). The good agreement with Fig. 2b of Ref [1] makes us confident with our implementation of the quasi-static formula.

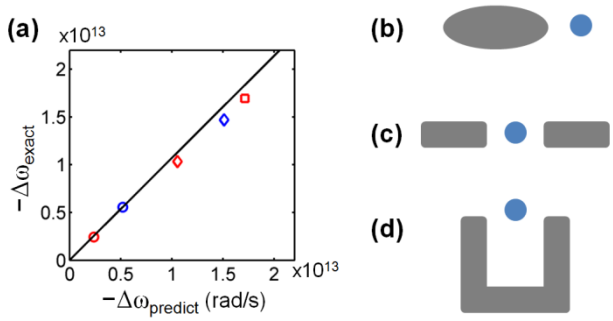

Figure S1. Test of our capability to correctly evaluate eq (S1) by reproducing Fig. 2b in [1]. Three silver resonators in air taken from Ref [1] are used. The perturbation (blue dot) is a silicon nanosphere (2.5-nm radius, n = 3.5) like in Ref [1]. (**a**) Peak frequency shifts for ellipsoid (circles), nanorod dimer (square) and SRR (diamonds). The black line has a slope of 1.07. (**b**) Sketch of the ellipsoid. The nanosphere is along the long-axis, with 3-nm (red circle) and 5-nm (blue circle) separation respectively. (**c**) Sketch of the nanorod dimer. The nanosphere is in the gap center. (**d**) Sketch of the SRR. The nanosphere is placed along the central axis, being 15 nm (red diamond) and 20 nm (blue diamond) above the bottom arm. A Drude model $\varepsilon_m = 4 - \omega_p^2 / \left(\omega^2 - i\omega\Gamma\right)$ is adopted for the relative permittivity of silver with ω_p = 1.4x10^{16} s^{-1} and Γ = 3.2x10^{13} s^{-1}.

Comparison. Reinforced by the agreement, we systematically compare the accuracy of the present master equation, based on quasi-normal mode (QNM) theory, and that of the quasi-static formula. For the comparison, we consider metallic resonators perturbed by a nanosphere. The resonators are silver ellipsoids (taken from [1]), gold nanorods and nanorod dimers (both taken from the main text). The resonator sizes are gradually increased, using a *scaling factor* (SF), from *deep* sub–λ *scale* (~λ/15) (similar to those in [1] and in Fig. S1) to ~λ/4. This size range is typically encountered in plasmonic sensing applications.

In fact, the quasi-static formula predicts complex-valued resonance shifts $\Delta\tilde{\lambda}$ as the metal permittivity ε_{ca} is complex and the perturbation permittivity (taken into account via α_{NP}) may be complex as well. So we provide the comparison for both *Re*($\Delta\tilde{\lambda}$) and *Im*($\Delta\tilde{\lambda}$), although no predictions of *Im*($\Delta\tilde{\lambda}$) are reported in Ref [1]. We emphasize that, though in plasmonic sensing the peak broadening is rarely considered, both peak broadening and shift are fundamental effects associated to a perturbed resonance, thus they should be treated together into a theoretical work, just like in previous works on high-Q RF and photonic cavities [2-4].

The resonance shifts, obtained with fully-vectorial calculations ($\Delta\tilde{\lambda}_{exact}$), with the quasi-static formula ($\Delta\tilde{\lambda}_{static}$) and with the master equation ($\Delta\tilde{\lambda}_{QNM}$), are compared in Figs. S2 (ellipsoid), S3 (nanorod), and S4 (dimer). We also compare the relative

errors, defined as the normalized difference between the exact and approximated values. $\Delta\tilde{\lambda}_{exact}$ is obtained as the difference between the complex-valued eigenwavelengths of the perturbed and the unperturbed QNMs. To provide a comparison as accurate as possible, consistently with eq (S1) and the work in [1], when using the master equation, we assume that the field in the perturbation is uniform and given by the field at the perturbation center.

Figs. S2, S3, and S4 evidence that the quasi-static formula cannot predict $Im(\Delta\tilde{\lambda})$ at all, and it is accurate for $Re(\Delta\tilde{\lambda})$ only at deep sub–λ scale, typically for SF ≤ 1.5. Such a small value sets a severe upper bound on the characteristic transverse size that can be considered with accuracy ($< \lambda/10$); for SF = 1.5, the surfaces of the nanorod and the ellipsoid are 2500 nm^2 and 3200 nm^2, respectively. They correspond to nanospheres with 25~30 nm diameters, being one or two orders of magnitude smaller than the typical surface areas used in biosensing applications [5,6]. Additionally note that absorption and scattering cross-sections become comparable when the nanospheres are about 60 nm in diameter for silver nanospheres and 80 nm in diameter for gold nanospheres.

On the other hand, predictions of both $Re(\Delta\tilde{\lambda})$ and $Im(\Delta\tilde{\lambda})$ made by the master equation are highly accurate at least up to SF = 4, with a relative error below 5% that is even decreasing as the nanoparticle sizes increase. We have check that increase of the relative error as the nanoparticle dimensions are scaled down is due to the fact that the QNM field varies over the perturbation for small nanoresonators and the polarizability model used for the comparison does not consider such variations. We have checked that by taking into account the variation as it is done in the main text.

Conclusion. The quasi-static formula could be only applicable for ultrasmall metallic resonators ($< \lambda/10$). The QNM-theory-based master equation is not limited by size and might be used for a broader variety of nanoparticles and realistic applications. As QNMs are the truly eigensolutions of Maxwell's equations, without approximations about resonator size, the master equation is valid independent of the resonator size.

Furthermore, concerning practical implementation, the QNM-based master equation and the quasi-static formula both require the computation of the resonance mode profile, and demand very similar computational loads. We also provide a robust numerical protocol for calculating and normalizing QNMs [8,9]. For metallic resonators of regular shapes and sizes (like for the examples shown here), it just consumes a few minutes to obtain a QNM with a low speed computational workstation equipped with a finite element software.

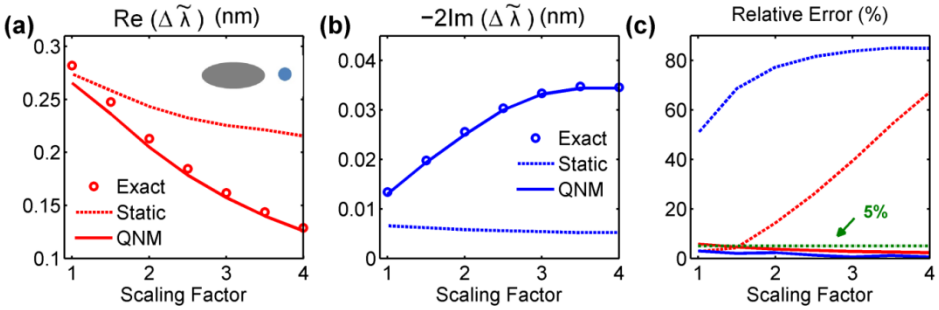

Figure S2. Resonance shifts of Ag ellipsoids in air perturbed by a silicon nanosphere (2.5-nm radius, *n* = 3.5), with a 5-nm separation (fixed). (**a**) and (**b**) *Re*($\Delta\tilde{\lambda}$) and −2•*Im*($\Delta\tilde{\lambda}$), as a function of the scaling factor, obtained with fully-vectorial simulations (circles), the quasi-static formula (dashed, denoted by *static*) and the master equation (solid, denoted by *QNM*). (c) Relative errors, defined as |exact − prediction|/|exact|, for the quasi-static formula (dashed) and the master equation (solid). Red and blue curves correspond to *Re*($\Delta\tilde{\lambda}$) and *Im*($\Delta\tilde{\lambda}$). The green line marks a 5% relative error. Scaling factor SF = 1 corresponds to the ellipsoid in [1], with 40-nm long axis and 14-nm short axes.

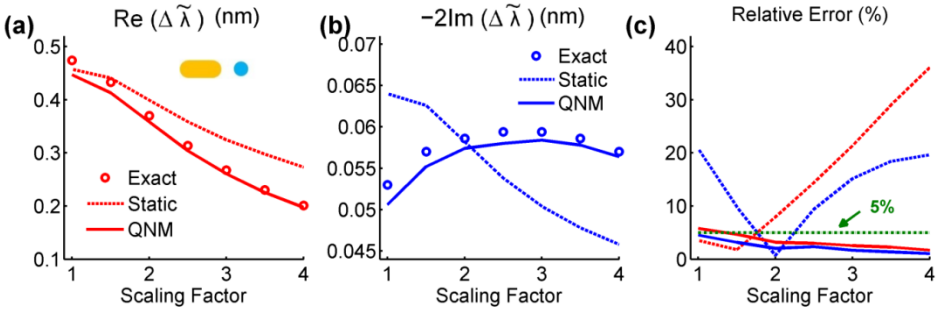

Figure S3. Same as in Fig. S2 except that gold nanorods are considered. The nanorods are immersed in water (*n* = 1.33) perturbed by a silicon nanosphere (3-nm radius, *n* = 3.5), with a 6-nm separation (fixed). Scaling factor SF = 1 corresponds to a nanorod with 5-nm radius and 30-nm length, and SF = 3 corresponds to the nanorod considered in Fig. 3 (main text).

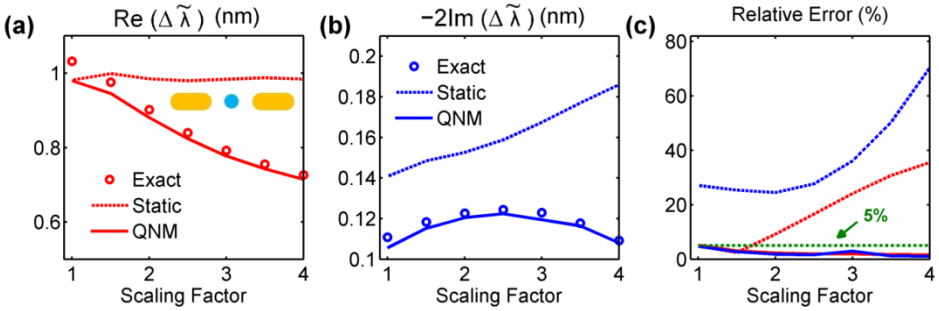

Figure S4. Same as in Fig. S2 except that gold nanorod dimers are considered. The dimers are immersed in water (*n* = 1.33) and perturbed by a protein nanosphere (5-nm radius, *n* = 1.5), placed at the gap center. Scaling factor SF = 1 corresponds to a dimer, with 15-nm gap between the two arms (5-nm radius and 30-nm length), and SF = 3 corresponds to the one considered in Fig. 3 (main text). The gap is fixed to be 15 nm for all scaling factors.

Table S1 lists all the eigenwavelengths $\tilde{\lambda}_m$ of the original QNMs associated to the resonators shown in Figs. S2 – S4.

Table S1. Eigenwavelengths $\tilde{\lambda}_m$ of Original QNMs (unit: nm)

Scaling Factor	Silver Ellipsoid	Gold Nanorod	Gold Nanorod Dimer
1.0	467.09 – 2.61*i*	620.75 – 14.77*i*	636.82 – 16.18*i*
1.5	476.31 – 4.48*i*	632.56 – 16.54*i*	660.14 – 19.96*i*
2.0	489.07 – 7.98*i*	648.54 – 19.73*i*	688.09 – 26.29*i*
2.5	505.25 – 13.43*i*	668.32 – 24.52*i*	720.31 – 35.36*i*
3.0	524.69 – 20.98*i*	691.52 – 30.94*i*	756.44 – 47.12*i*
3.5	547.31 – 30.58*i*	717.74 – 38.89*i*	796.24 – 61.24*i*
4.0	572.97 – 42.02*i*	746.68 – 48.26*i*	839.51 – 77.53*i*

2. Analysis of the errors induced by the approximations made to derive the Master Equation

The master equation eq 1 (main text) is derived by applying two approximations into eq 3, which is directly derived by applying Lorentz reciprocity to the original and perturbed modes $(\tilde{\mathbf{E}},\tilde{\mathbf{H}})$ and $(\tilde{\mathbf{E}}',\tilde{\mathbf{H}}')$ and therefore offers the *exact* shift $\Delta\tilde{\omega}_{exact}$. Hereafter we analyze the impact of the approximations on the prediction accuracy.

For the sake of clarity, we rewrite eq 3 as

$$\frac{\Delta\tilde{\omega}}{\tilde{\omega}} = -\frac{N_{\text{exact}}}{D_{\text{exact}}}, \tag{S2}$$

where N_{exact} and D_{exact} respectively denote the numerator and denominator of the right-hand side of eq 3. To derive the master equation that requires the sole knowledge of the original mode $(\tilde{\mathbf{E}},\tilde{\mathbf{H}})$, we use **two approximations**:

(**i**) in the denominator,

$$D_{\text{exact}} = \iiint_{\Omega}\left\{\tilde{\mathbf{E}}(\mathbf{r})\cdot\frac{\partial[\omega\boldsymbol{\varepsilon}(\mathbf{r},\omega)]}{\partial\omega}\tilde{\mathbf{E}}'(\mathbf{r}) - \tilde{\mathbf{H}}(\mathbf{r})\cdot\frac{\partial[\omega\boldsymbol{\mu}(\mathbf{r},\omega)]}{\partial\omega}\tilde{\mathbf{H}}'(\mathbf{r})\right\}d^3\mathbf{r}\ , \tag{S3}$$

we replace $(\tilde{\mathbf{E}}',\tilde{\mathbf{H}}')$ by the normalized original mode $(\tilde{\mathbf{E}},\tilde{\mathbf{H}})$, thus D_{exact} becomes

$$D_{appr} = \iiint_{\Omega}\left\{\tilde{\mathbf{E}}\cdot\frac{\partial[\omega\boldsymbol{\varepsilon}]}{\partial\omega}\tilde{\mathbf{E}} - \tilde{\mathbf{H}}\cdot\frac{\partial[\omega\boldsymbol{\mu}]}{\partial\omega}\tilde{\mathbf{H}}\right\}\mathrm{d}^3\mathbf{r} = 1;$$

(**ii**) in the numerator,

$$N_{\text{exact}} = \iiint_{V_p}\Delta\boldsymbol{\varepsilon}(\mathbf{r},\tilde{\omega})\tilde{\mathbf{E}}'(\mathbf{r})\cdot\tilde{\mathbf{E}}(\mathbf{r})d^3\mathbf{r}\ , \tag{S4}$$

we replace $\tilde{\mathbf{E}}'$ by the modified version $\tilde{\mathbf{E}}_{app}$ of $\tilde{\mathbf{E}}$.

We evaluate the errors due to approximations (**i**) and (**ii**) for an example shown in Fig. 3b (main text), in which a gold nanorod is perturbed by a gold nanosphere (3-nm

radius). The example is selected because the predicted shifts $\Delta\tilde{\omega}_{predict}$ show particularly large (compared to other examples) deviations from the exact shifts $\Delta\tilde{\omega}_{exact}$, especially for small nanorod-nanosphere separation distances (≤ 1 nm).

Denominator errors. Figure S5(a) shows the relative error $\left|D_{appr}-D_{exact}\right|/\left|D_{exact}\right|$ made on the denominator by replacing D_{exact} by D_{appr} as a function of the separation. Actually, the relative error $\left|D_{appr}-D_{exact}\right|/\left|D_{exact}\right|$ is less than 1% for separations as small as 0.5 nm. Therefore the replacement of $\left(\tilde{\mathbf{E}}',\tilde{\mathbf{H}}'\right)$ by $\left(\tilde{\mathbf{E}},\tilde{\mathbf{H}}\right)$ in the denominator, i.e. approximation (**i**), introduces negligible errors, which are comparable to the ratio between the perturbation volume and the mode volume.

Numerator errors. For approximation (**ii**), two versions can be applied: (**A**) a crude one $\tilde{\mathbf{E}}_{app}=\tilde{\mathbf{E}}$ and (**B**) $\tilde{\mathbf{E}}_{app}=\boldsymbol{\alpha}\varepsilon_b\tilde{\mathbf{E}}/\left[V_p\,\Delta\boldsymbol{\varepsilon}(\mathbf{r},\tilde{\omega})\right]$ (adopted in the main text), which incorporates local field correction [10]. Let's denote the corresponding numerator as N_{appA} and N_{appB}, respectively. Figures S5(b) and S5(c) show $Re(\Delta\tilde{\lambda})$ and $-2Im\bullet(\Delta\tilde{\lambda})$, calculated with combinations $\left(N_{\text{appA}},D_{\text{appr}}\right)$ (black squares), $\left(N_{\text{appB}},D_{\text{appr}}\right)$ (green triangles) and $\left(N_{\text{exact}},D_{\text{exact}}\right)$(red curve). We have checked that, consistently with Fig. S5(a), predictions obtained with the combination $\left(N_{\text{exact}},D_{\text{appr}}\right)$ are superimposed with the exact values and not shown for the sake of clarity. Predictions obtained using $\left(N_{\text{appA}},D_{\text{exact}}\right)$ show large errors and evidence the need to apply local field corrections. However $\left(N_{\text{appB}},D_{\text{appr}}\right)$ leads to much more accurate predictions. Note that it is this combination that is used to obtain the data in Fig. 3 (main text).

Considering the negligible error in the denominator, the stringent deviation between predictions obtained by $\left(N_{\text{appB}},D_{\text{appr}}\right)$ and exact values for small separations (≤1 nm) indicates that local-field corrections cannot offer accurate estimation of $\tilde{\mathbf{E}}'$ for some extreme cases. Careful observation (not shown here) of $\tilde{\mathbf{E}}'$ for separations smaller than 1 nm revealed the formation of an intense gap plasmon, tightly confined between the gold nanorod (nanoparticle) and the gold nanosphere (perturbation).

Summary. The evaluation evidences that the major approximation used for deriving the master equation arises from the replacement of $\tilde{\mathbf{E}}'$ by $\tilde{\mathbf{E}}_{app}$ in the numerator of eq 3 (main text) and that it is necessary to use local field correction for high accuracy. In contrast, the error introduced by approximation (**i**), i.e. the replacement of $\left(\tilde{\mathbf{E}}',\tilde{\mathbf{H}}'\right)$ by $\left(\tilde{\mathbf{E}},\tilde{\mathbf{H}}\right)$ in the denominator of eq 3, is negligible.

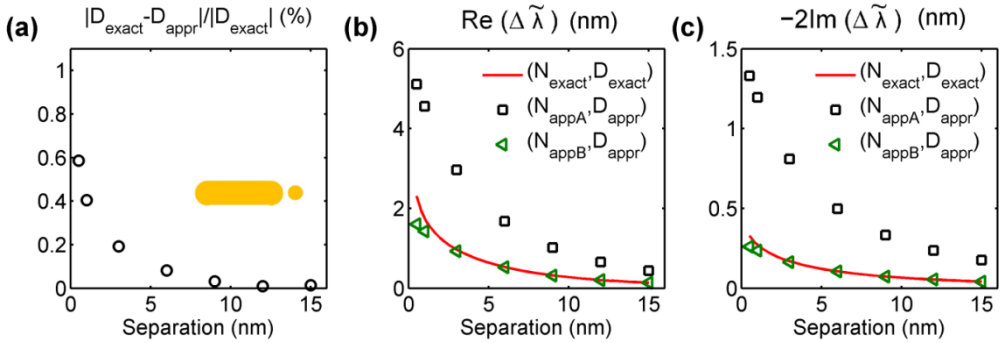

Figure S5. Errors introduced by applying approximations (i) and (ii) into eq 3 (main text) for the derivation of the master equation (main text). The errors are estimated for a gold nanorod perturbed by a gold nanosphere (inset) as a function of the nanorod-nanosphere separation. **(a)** $\left|D_{appr}-D_{exact}\right|/\left|D_{exact}\right|$. **(b)** and **(c)** Resonance shifts, *Re*($\Delta\tilde{\lambda}$) and –2•*Im*($\Delta\tilde{\lambda}$), obtained with combinations $\left(N_{appA},D_{appr}\right)$ and $\left(N_{appB},D_{appr}\right)$ are shown with black squares and green triangles. The exact value, corresponding to $\left(N_{exact},D_{exact}\right)$, is shown with the red curve.

References.

(1) Zhang, W; Martin, O. J. F. *ACS Photonics* **2015**, 2 (1), pp 144–150.

(2) Waldron, R. A. *Proc. Inst. Electr. Eng.* **1960**, 107C, 272.

(3) Inoue, R.; Kitano, H.; Maeda, A.; *J. Appl. Phys*. **2003**, 93, 2736.

(4) Koenderink, A. F.; Kafesaki, M.; Buchler, B. C.; Sandoghdar, V. *Phys. Rev. Lett*. **2005**, 95, 153904.

(5) Anker, J.; Paige Hall, W.; Lyandres, O.; Shah, N.; Zhao, J.; Van Duyne, R. P. *Nat.Mat*. **2008**, *7*, 442 - 453.

(6) Ament, I.; Prasad, J.; Henkel, A.; Schmachtel, S.; Sönnichsen, C. *Nano Lett*. **2012**,*12*, 1092−1095.

(8) Bai, Q.; Perrin, M.; Sauvan, C.; Hugonin, J.-P.; Lalanne, P. Opt. Exp. **2013**, 21, 27371-27382.

(9) see the webpage: https://www.lp2n.institutoptique.fr/Membres-Services /Responsables-d-equipe/LALANNE-Philippe

(10)Harrington, R. F. Time-Harmonic Electromagnetic Fields; Chapter 7, Wiley-IEEE Press, September 2001.